Deep-Sea Research II 120 (2015) 114–123

Contents lists available at ScienceDirect

Deep-Sea Research II

journal homepage: www.elsevier.com/locate/dsr2

Characteristics of mesozooplankton sound-scattering layer in the Pacific Summer Water, Arctic Ocean

Hyoung Sul La [a,*], Myounghee Kang [b], Hans-Uwe Dahms [c], Ho Kyung Ha [d], Eun Jin Yang [a], Hyungbeen Lee [e], Young Nam Kim [f], Kyung Ho Chung [a], Sung-Ho Kang [a]

[a] Korea Polar Research Institute, Incheon 406-840, Republic of Korea
[b] Gyeongsang National University, Tongyeong 650-160, Republic of Korea
[c] Kaohsiung Medical University, Kaohsiung 80708, Taiwan, ROC and National Sun Yat-sen University, Kaohsiung 80424, Taiwan, ROC
[d] Department of Ocean Sciences, Inha University, Incheon 402-751, Republic of Korea
[e] National Fisheries Research and Development Institute, Republic of Korea
[f] Korea Marine Environment Management Corporation, Seoul 135-870, Republic of Korea

ARTICLE INFO

Available online 14 January 2015

Keywords:
Arctic Ocean
Canada Basin
Northwind Ridge
Sound-scattering layer
Arctic copepods
Eddy
Pacific Summer Water

ABSTRACT

This study investigated the variations in the sound-scattering layer (SSL) that were reflected from the mesozooplankton communities around the Northwind Ridge in the western Arctic Ocean. A multi-frequency acoustic survey was conducted to reveal the SSL distribution dominated by Arctic copepods in the early summer of 2010. The SSL distribution was well correlated with the salinity, nutrients and chlorophyll *a* (chl-*a*) associated with the features of the Pacific Summer Water (PSW). The SSL was observed primarily in the uppermost 100 m of the PSW, which provided a desirable habitat for Arctic copepods due to high nutrients and phytoplankton biomass. The highest density SSL was observed in the eddy-like structure of the PSW, which is most likely because of the high nutrients and chl-*a*. High regional densities in the SSL indicated that Arctic copepods provide a large portion of the biomass and contribution to the food webs in the PSW, in the western Arctic Ocean.

1. Introduction

Mesozooplankton play a key role in the pelagic food webs of the Arctic Ocean and have a large influence on the energy flow and function of productive marine ecosystems (Riser et al., 2008). In the Arctic mesozooplankton are predominantly comprised of calanoid copepods (Kosobokova and Hopcroft, 2010). Arctic copepods are rich in lipids and represent an important food source for other zooplankton species, pelagic fish such as polar cod (*Boreogadus saida*) (Lonne and Gulliksen, 1989); capelin (*Mallotus villosus*) (Hassel et al., 1991); and seabird species, such as the little auk (*Alle alle*) (Weslawski et al., 1999). Some Arctic copepods species feed on shelf-derived primary production sources (Plourde et al., 2005) and require mechanisms to return to their pelagic environments to undergo diapause (Conover, 1988; Cottier et al., 2006). Although pelagic Arctic copepods are of major importance in Arctic food webs, their pathways and quantitative roles in the Arctic ecosystem are still not well known (Iken et al., 2010). Some Arctic copepods visit offshore to complete their life cycle. Therefore, variability in offshore transport can play an important role in modifying the shelf and basin ecosystems.

In the vicinity of the Northwind Ridge, water masses of the Pacific and Arctic Ocean undergo unique mixing patterns leading to changes in the Arctic ecosystem (Grebmeier and Harvey, 2005). This mixing involves wind-forced upwelling events (Munchow and Carmack, 1997) and small-scale eddies, which bring episodic pulses of nutrients into the euphotic zone and can thus affect the primary production (Benitez-Nelson et al., 2007). The Canada Basin includes numerous subsurface eddies in the halocline of Pacific-origin water (Manley and Hunkins, 1985; Muench et al., 2000; Honjo et al., 2010; Nishino et al., 2011). In addition, anomalous sea-ice reductions have been observed during the summer months, with spatial patterns that are unusual for the western Canada Basin (Maslanik et al., 1999; Shimada et al., 2006). The ice reduction is thought to be caused primarily by an increased flow of warm Pacific Summer Water (PSW) from the Bering Strait into the Arctic Ocean (Shimada et al., 2006; Woodgate et al., 2012). The lateral exchange of biological, chemical, and physical properties can impact the shelf-basin exchange mechanism (Walsh, 1995). Therefore, this region can be used as a natural laboratory to assess the relationship between the ecological characteristics of Arctic copepods and changes in environmental conditions related to the mid-ocean warm eddy of PSW. In addition, few studies have attempted to describe the response of

* Correspondence to: Division of Polar Ocean Environment, Korea Polar Research Institute, Korea Institute of Ocean Science and Technology, Incheon 406-840, Korea. Tel.: +82 32 760 5342; fax: +82 32 760 5399.
E-mail address: hsla@kopri.re.kr (H.S. La).

http://dx.doi.org/10.1016/j.dsr2.2015.01.005
0967-0645/

Arctic copepods communities to the passage of mesoscale warm eddies in the western Arctic Ocean.

In this study, acoustic methods were used to observe the horizontal and vertical distribution of SSL, which is dominated by Arctic copepods. The SSL represents a concentrated layer of marine organisms such as zooplankton aggregates and nekton that occur at specific depths (Zimmerman and Biggs, 1999; Benoit-Bird and Au, 2004; McManus et al., 2008). Acoustic system, which has been ubiquitously used, is considered to be the best tool for observing the spatial and temporal patterns of the vertical distribution of marine organisms (Clay and Medwin, 1977). Acoustic surveys can reflect the distribution of the most abundant species (Santora et al., 2011), and sample large volumes of water more rapidly than net sampling (Flagg and Smith, 1989). The target identities can be verified by net sampling (Foote and Stanton, 2000).

We conducted an acoustic survey using a multi-frequency acoustic system in the early summer of 2010 to observe variations in the SSL of Arctic copepods around the Northwind Ridge in the western Arctic Ocean. Our goal was to address the vertical and spatial distribution of Arctic copepods in relation to environmental conditions, including the physical and biogeochemical parameters of the PSW, and the existence of a mode-water eddy with warm core.

2. Materials and methods

The study was undertaken between 25 July and 2 August 2010 onboard the IBRV *Araon* (Fig. 1). The stations between 5 and 27 were used to detect warm water eddies between the Northwind Ridge and the Canada Basin. Acoustic, hydrographic (temperature and salinity), chemical (nutrients), and biological (chl-*a*) data were collected at each station (Table 1). Most stations were covered with sea ice except between St. 7 and 9. The presence of sea ice was defined as a region with sea ice covering more than 10% of the area (Arrigo et al., 2012).

2.1. Hydrographic data

At each station, conductivity-temperature-depth (CTD) measurements in the water column were recorded using a SeaBird 911+ sensor. An oxygen sensor was connected to the CTD system for dissolved oxygen measurements. All data were averaged into 1-m depth intervals to eliminate undesirable noise.

Water samples were analyzed for nutrients and chl-*a*. Discrete water samples were collected at each CTD station for nutrients (nitrate+nitrite, phosphate, silicate, and ammonium). Nutrients were analyzed with water samples collected at 0-, 5-, 10-, 15-, 20-, 25-, 35-, 50-, 70-, 90-, and 110-m depths using CTD-mounted Niskin water samplers. Nutrient analyses were performed using a Seal Analytical QuAAtro Autoanalyser connected to an autosampler with QuAAtro multitest methods and general absorptiom etry nitrate+nitrite (Armstrong et al., 1967), phosphate and sili cate (Grasshoff et al., 1983). Chl-*a* measurements were recorded at most stations (St. 5, 6, 8, 10, 13, 14, 16, 18, 21, 23, 25 and 27) using a fluorometer (TD-700, Turner Design Co.) after filtration through GF/F filters (24 mm) (Parsons et al., 1984).

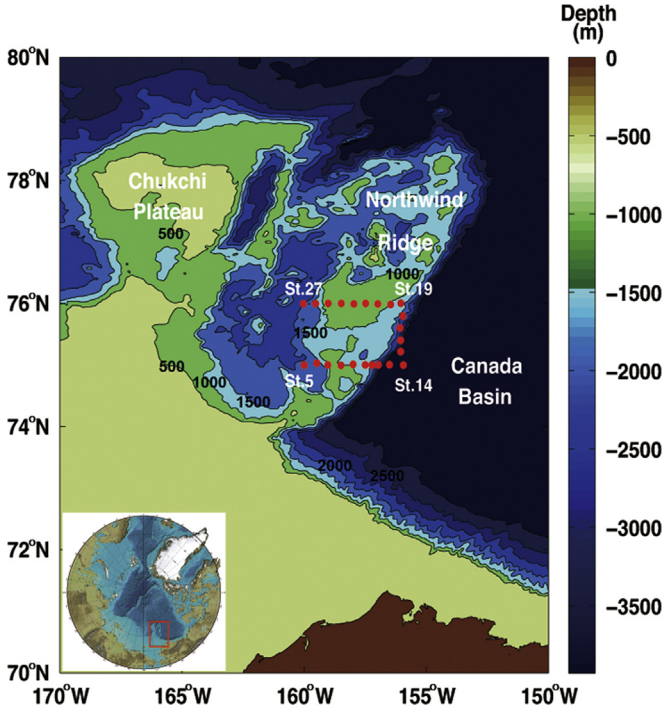

Fig. 1. Study area showing the acoustic, CTD, and net stations on the bathymetry.

Table 1
Sampling station details including start date and time, station location, maximum water depth, and sea ice cover. The sea ice concentration was derived from SSM/I data and averaged during the survey period of July 25–August 2 in 2010.

Station	Date (DD/MM/YYYY)	Start time (UTC)	Stop time (UTC)	Latitude (N)	Longitude (E)	Depth (m)	Sea ice concentration (%)
5	25/07/2010	16:21	18:00	75.000	160.000	2000	28.5
6	26/07/2010	17:11	18:35	75.028	159.475	1840	43.4
7[a]	27/07/2010	0:03	0:46	75.001	159.033	1110	6.6
8[a]	27/07/2010	3:35	4:15	74.994	158.494	950	9.1
9	27/07/2010	16:15	17:37	75.007	157.999	1030	6.6
10[a]	27/07/2010	20:37	21:27	75.002	157.508	1300	53.8
11[a]	28/07/2010	2:07	3:09	74.999	157.221	1550	46.5
12[a]	28/07/2010	4:57	6:48	75.003	156.966	2350	53.8
13	28/07/2010	9:20	11:10	75.004	156.503	3900	53.8
14[a]	29/07/2010	3:29	6:59	75.000	155.942	3904	71.5
15[a]	29/07/2010	22:53	1:23	75.216	156.047	3890	72.8
16	30/07/2010	5:20	7:23	75.401	156.048	2800	73.9
17	30/07/2010	17:15	19:18	75.600	156.074	2490	74.3
18[a]	31/07/2010	22:34	23:34	75.795	155.959	2050	75.4
19[a]	31/07/2010	4:27	5:28	76.003	156.039	1280	74.1
20[a]	31/07/2010	21:20	21:50	75.984	156.458	1080	72.4
21[a]	1/08/2010	0:43	1:15	75.992	156.992	940	73.2
22	1/08/2010	12:00	12:47	76.000	157.483	620	76.4
23	1/08/2010	15:40	16:03	75.990	157.970	520	79.6
24[a]	1/08/2010	21:06	21:25	76.001	158.479	540	78.5
25[a]	2/08/2010	0:02	0:41	76.002	159.013	820	78.1
26	2/08/2010	5:55	8:03	75.999	159.531	1540	80.2
27	2/08/2010	17:01	17:50	75.993	160.032	2100	82.6

[a] Night (Rabindranath et al., 2011).

2.2. Net sampling

Mesozooplankton were collected with a NORPAC Bongo net (mouth area of 0.5 m^{-2}, 200-μm mesh) that was hauled vertically from 200 m to the surface. The nets were used to verify the composition of the SSL recorded in the echograms. Data were collected from 12 sampling stations and analyzed for mesozooplankton composition at 7 stations (St. 6, 8, 13, 16, 21, 25 and 27). The plankton catches were preserved with 4% borate-buffered formaldehyde and analyzed under a stereo-microscope after the cruise.

In the laboratory, each sample was split with a Folsom splitter into sub-samples of less than 500 individuals for taxonomic identification and counting. The species composition of each sample was determined by counting all mature animals in each sub-sample. Keys and taxonomic references were used for copepod identification. Sorting and identification of zooplanktons samples were carried out as described by Falk-Petersen et al. (2008). The following taxonomic references were used: Sirenko (2001), Bucklin et al. (2010), Hopcroft et al. (2010), and Dvoretsky and Dvoretsky (2010). The copepod abundance (individuals m^{-3}) was calculated from eight CTD stations (St. 6, 8, 10, 13, 16, 21, 25, and 27) using a known volume filtered through a 330-μm mesh net, and quantified by the revolution counts of a flow meter attached to the center of the net mouth.

2.3. Acoustic measurements and analysis

Acoustic data were collected using a Simrad EK60 scientific echosounder system configured with a 38- and 120-kHz split-beam transducer. Transmission of pings and logging of the received signals was controlled using the Simrad ER60 software v. 2.0.0. The power settings were set to maximum, and the signal was transmitted at each frequency every 2 s with a pulse length of 1 ms. Other acoustic instruments were turned off to minimize frequency interferences. At all stations, the ship remained stationary for approximately 2–10 h, while the volume backscattering strengths (S_v, dB re 1 m^{-1}) were collected in conjunction with CTD measurements and net castings. The echosounder was calibrated at all frequencies after the cruise.

The raw data files of the EK60 echosounder for 38 and 120 kHz were imported into the Echoview (ver. 5.3) acoustic data analysis software (Myriax, 2012). Data for the uppermost 200 m of the water column from the top were used to compare with eddy signatures. The background noise, which was amplified in the process of applying time-varied-gain (TVG) compensation to calculate the S_v, increased with increasing water depth. Therefore, a weak signal, for example, similar to that of plankton, can be buried in relatively deep water because of accumulated background noise. The noise level depends on the distance from the transducer and can be removed using the time-varied threshold (TVT) function, as originally conceptualized by Watkins and Brierley (1996). The TVT function was applied to every ping for all S_v values at 38 and 120 kHz (Myriax, 2012). The TVT function is expressed in the following equation:

$$TVT(r) = S_v + 20\log(r) + 2\alpha(r-1) \quad (1)$$

where S_v is the volume backscattering strength at 1 m depth, r is the distance from the transducer (m), and α is the absorption coefficient (dB m^{-1}). The value of S_v is determined by examining the signal, with respect to the recording of noise, and fitting a TVG curve to it. Background noise can then be subtracted by using the TVT values in the linear domain from the original S_v values. Occasionally, non-biological signals, such as surface bubbles, the sea bottom, and false bottom echoes, were identified and manually excluded as bad data. The noise-filtered data were subsequently resampled into bins with dimensions of 1-m depth by 50 pings.

Multi-frequency techniques have been widely used to classify the acoustic backscatter for species classification (Madureira et al., 1993; Brierley and Watkins, 1996; Brierley et al., 1998; CCAMLR, 2010; Rabindranath et al., 2011; Fielding et al., 2012; La et al., 2015). The

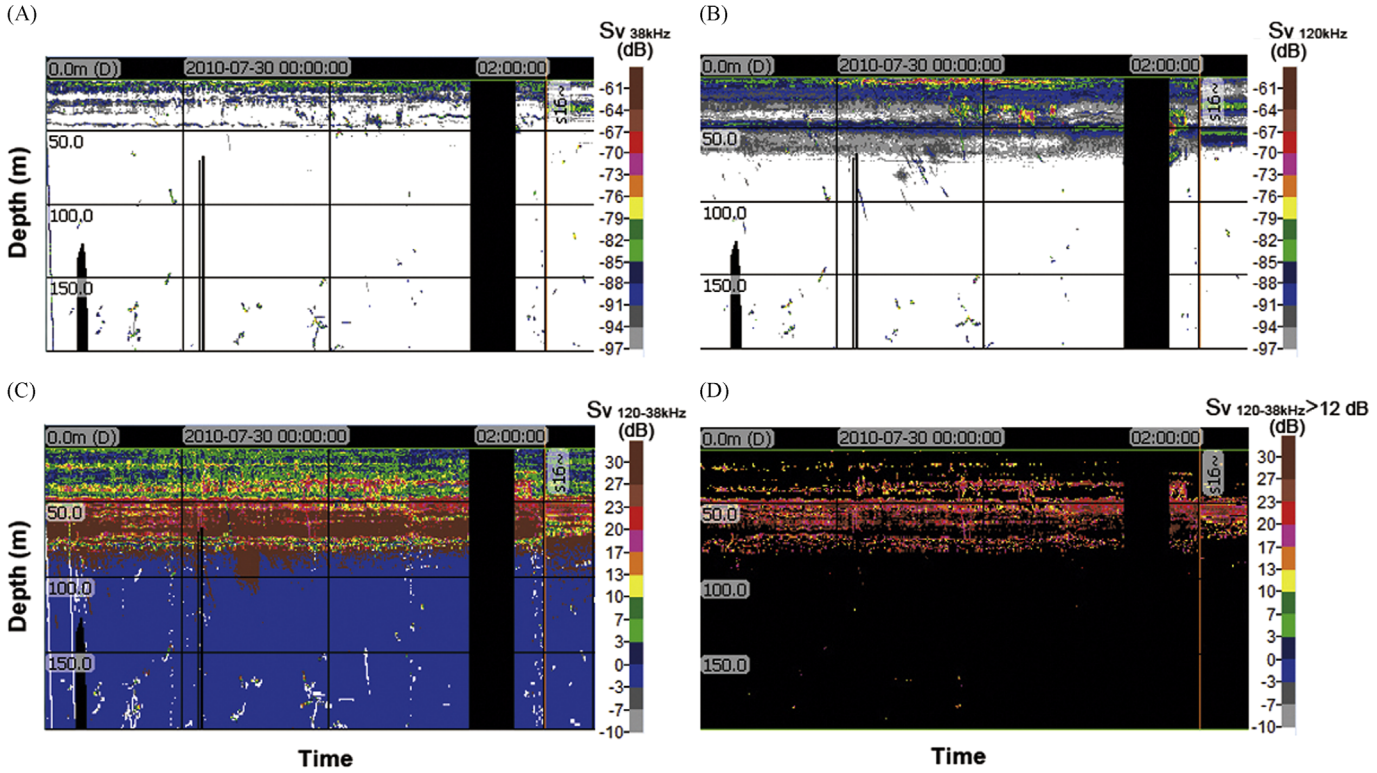

Fig. 2. The S_v echograms at 38 (a) and 120 kHz (b), the dB difference echogram (c), the 120 kHz S_v echogram that includes only Copepod by using the dB difference window of >12 dB (d). This was made using the data around St. 15. The black band on the top was considered as no-data due to the presence of a non-biological noise containing ring down noise on the water surface. The vertical black band was made because some noise contaminated the data in that water column.

two-frequency dB difference (the difference in volume backscattering strength values at two frequencies) can be obtained by the following equation (Kang et al., 2002):

$$\Delta S_v = S_v(f_2) - S_v(f_1) \quad (2)$$

where S_v is the volume backscattering strength, and f_1 and f_2 are 38 and 120 kHz, respectively. To discriminate among three size groups of zooplankton, we defined appropriate windows for the dB difference (Madureira et al., 1993; Rabindranath et al., 2011). Mesozooplankton was defined by a ΔS_v window of >12 dB, macrozooplankton/micronekton was defined by a ΔS_v window of $2-12$ dB, and fish (with swim bladders) was defined by a ΔS_v window of <2 dB. The representative echograms of 38 and 120 kHz S_v are shown in Fig. 2. The 120 kHz S_v echogram including only mesozooplankton was made using bitmap and mask features (Fig. 2d). Bitmap echogram was made on the basis of the ΔS_v window of >12 dB. For example only if echoes of dB difference echogram were larger than 12 dB, they became "true" otherwise "false". Then, echoes on the original S_v echogram corresponding to "false" were masked using mask operator. Accordingly only echoes that is "true", which met the ΔS_v window, were left on the S_v echogram. The acoustic density in a specific layer was indicated through the nautical area scattering coefficient (s_A, $m^2\,nmi^{-2}$) for backscattering (Simmonds and MacLennan, 2005). The 120 kHz S_v attributed to mesozooplankton by the dB difference was integrated from 10 m below transducer to 200 m and averaged for approximately 2 h during each CTD cast to determine an appropriate scale for analysis. The s_A was exported into Matlab® for further analysis to demonstrate the abundance and distribution of the sound-scattering organisms. For analysis the wei ghted mean depth (WMD) of scattering layer was calculated to find main depth of SSL for each station to observe the variability of the main scattering layer in the echogram (Roe et al., 1984).

3. Results

3.1. Characteristics of the water masses

At each station, the water column was characterized by a complex layering of water masses. The potential temperature–salinity diagram revealed the presence of four water masses, Surface Mixed Water (SMW), PSW, Pacific Winter Water (PWW), and Atlantic Water (AW) (Fig. 3). The presence of these water masses is typical for the Arctic Ocean (Honjo et al., 2010). The water column here is commonly stratified with a strong pycnocline between the SMW, which has a low temperature and salinity and the PSW, which has a high temperature and salinity. The salinity of the SMW dropped down to 26 psu in the upper layer (from the surface to 40-m depth), being affected by freshening from sea ice melts and terrestrial freshwater input (Honjo et al., 2010). The salinity of the PSW ranges from 30 to 32.5 psu between 40 and 150 m. The PWW and AW occupied the underlying layers. For these masses, we focused on the upper 200 m of the water column to reveal eddy signatures.

Along-track sections derived from hydrographic observations demonstrated the impact of eddies on the vertical structure of the physical and biogeochemical properties (Fig. 4). A strong halocline was observed between SMW and PSW, with salinities ranging from 30 to 31 psu at depths of approximately 20–40 m. At low prevailing temperatures, the temperature effect of density was small. Salinity was, therefore, the primary factor determining density stratifica tion. At most stations, the SMW ranged from 1.5 to -0.7 °C, with salinities ranging from 26 to 30 psu between the surface and 40 m underwater. The PSW ranged from -0.9 to 0.5 °C, with salinities ranging from 30 to 32.5 psu between 40- and 100-m depth.

The vertical structure of the water column can be used to identify the location of mesoscale eddies in the ocean (McGillicuddy et al., 1999). The vertical profiles of the halocline within eddies provide indirect evidence of upwelling and downwelling. The features observed at both St. 8 and 13 are reminiscent of "mode-water eddies" which displace the seasonal pycnocline upward and the main thermocline downward (McGillicuddy et al., 1999). These mode-water eddies had mesoscale horizontal dimensions (25–50 km). The eddy around St. 8 (E1) was composed of a thick lens of warm water, which elevated the seasonal halocline (i.e., the 30-psu isohaline) and depressed the main halocline (i.e., the 32.5-psu isohaline). The maximum temperature of the eddy was 0.5 °C at the center. The eddy around St. 13 (E2) was also composed of a thick lens of warm water with doming of the seasonal halocline and downward deflection of the main halocline. The uplift of the seasonal halocline was stronger than that around St. 8. The maximum temperature was approximately 0.1 °C around the seasonal halocline.

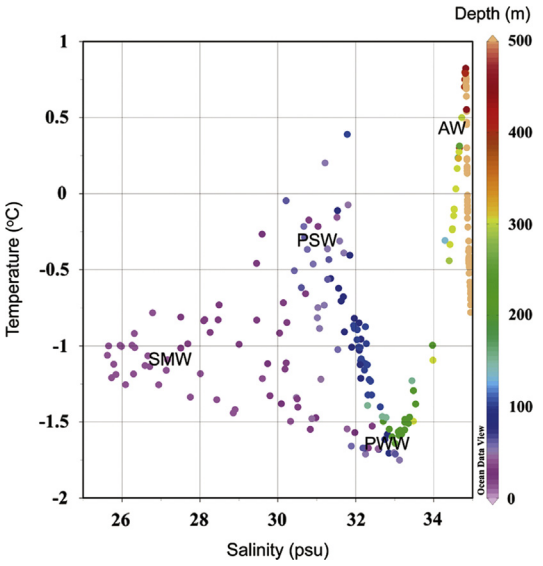

Fig. 3. The potential temperature–salinity diagram. It characteristics that correspond to the Surface Mixed Water (SMW), the Pacific Summer Water (PSW), the Pacific Winter Water (PWW), and the Atlantic Water (AW).

3.2. Vertical distribution of nutrients and chl-a

The upper ocean nutrient distribution reflects the perturbations in the halocline caused by the underlying mode-water eddy features. Ammonium showed a low concentration of <1 μmol L^{-1} at most stations. Phosphate, nitrate+nitrite and silicate concentrations were relatively depleted in the surface waters, and increased gradually with depth at all stations. However, the vertical distributions were somewhat different between E1 and E2. For E1, the phosphate, nitrate+nitrite and silicate tended to be depressed along with the main halocline, rather than elevated with the seasonal thermocline. In E2, the phosphate, nitrate+nitrite and silicate were clearly elevated to a depth of 50 m by eddy-induced upwelling at the seasonal halocline.

A distinct characteristic of the vertical distribution of chl-*a* was the pronounced subsurface chlorophyll maximum (SCM) near the base of the euphotic zone. Both the magnitude and vertical depth of the high chl-*a* were significantly affected by the presence of an eddy with strong upwelling. High chl-*a* (3.6 μg L^{-1}) was observed at a depth of 50 m at St. 13, where strong doming of the seasonal thermocline in E2 was observed. The SCM layer, with a chl-*a* concentration of <1 μg L^{-1}, was observed at the other stations. The depth-integrated chl-*a* concentration was estimated to be 6.2 μg m^{-2} at St. 13, which was an order of magnitude greater than the concentrations at the other stations.

3.3. Net samplings

We identified the major mesozooplankton groups around the Northwind Ridge. The mesozooplankton population was dominated by calanoid copepods during the summer period (Table 3). St. 13 had higher proportions of Copepoda (93.6%) and Ostracoda (2.9%) than other mesozooplankton groups, making this station a distinct group. A cluster analysis based on a Bray Curtis similarity analysis using values of proportion (Table 3) showed that for all stations, except St. 13, the composition of copepods was very similar. The similarity index was higher than 97.7%. This distribution occurred because the dominant taxon (the copepods) was present at higher proportions (> 89.8%) in all samples. Copepod assemblages are also investigated and described in more detail in a separate contribution to this volume. Three large Arctic calanoid copepods (*Calanus hyperboreus*, *Calanus glacialis*, and *Metridia longa*) dominated at most stations, which is similar to results from the western Arctic Ocean (Longhurst et al., 1984; Conover and Huntley, 1991; Falk-Petersen et al., 1999; Kosobokova and Hirche, 2000; Auel and Hagen, 2002; Ashjian et al., 2003; Campbell et al., 2009). The mean prosome length of Arctic copepods was 7 mm (S.D. = 0.7), which was 60% larger than other mesozooplankton.

3.4. Distribution of Arctic copepods

Vertical patterns of the SSL from the mesozooplankton indicated that there was a relatively uniform distribution over the study area (Fig. 5). The SSL was primarily created by the relatively higher densities of Arctic copepods, and its distribution within the PSW was between 20 and 100 m at all stations. The vertical distributions of the SSL were related to features of the hydrographic structure of the water column such as the existence of the mode-water warm eddy. The SSL was observed mainly at depths from 20 to 40 m in both the E1 and E2, where the seasonal halocline surfaces were domed upward. The SSL was distributed between 30 and 60 m at the other stations. There was no indication of an upward movement towards the SMW.

The s_A, which was attributed to Arctic copepods, also exhibited the distinct spatial variability associated with the existence of the mode-water warm eddy (Fig. 6). The s_A was significantly higher around E2 than at the other stations within the surveyed region and the highest s_A (17.4 m^2 nmi^{-2}) was observed at St. 13. The mean s_A at stations in the E2 (St. 10–13) was 15.2 m^2 nmi^{-2}, which was approximately eightfold higher than the mean densities at the other stations. The WMD of the SSL was distributed at depths from 30 to 55 m and the most of WMD appeared to be deeper than 40 m. However, the WMD clearly increased at depths of 30–35 m around E2. The seasonal halocline showed a similar pattern to s_A and WMD, increasing at shallower depths around E2. Diel migration can influence the vertical distribution of s_A and WMD variability due to diurnal migration because the acoustic data were recorded during all periods of the day and night. However, the mean s_A and WMD at each echogram did not show diel variation between day and night (Table 1 and Fig. 6). The results indicated no significant differences in s_A and WMD between day and night (Mann–Whitney *U*-test, $p < 0.01$). Given the lack of evidence of diel migration, we could

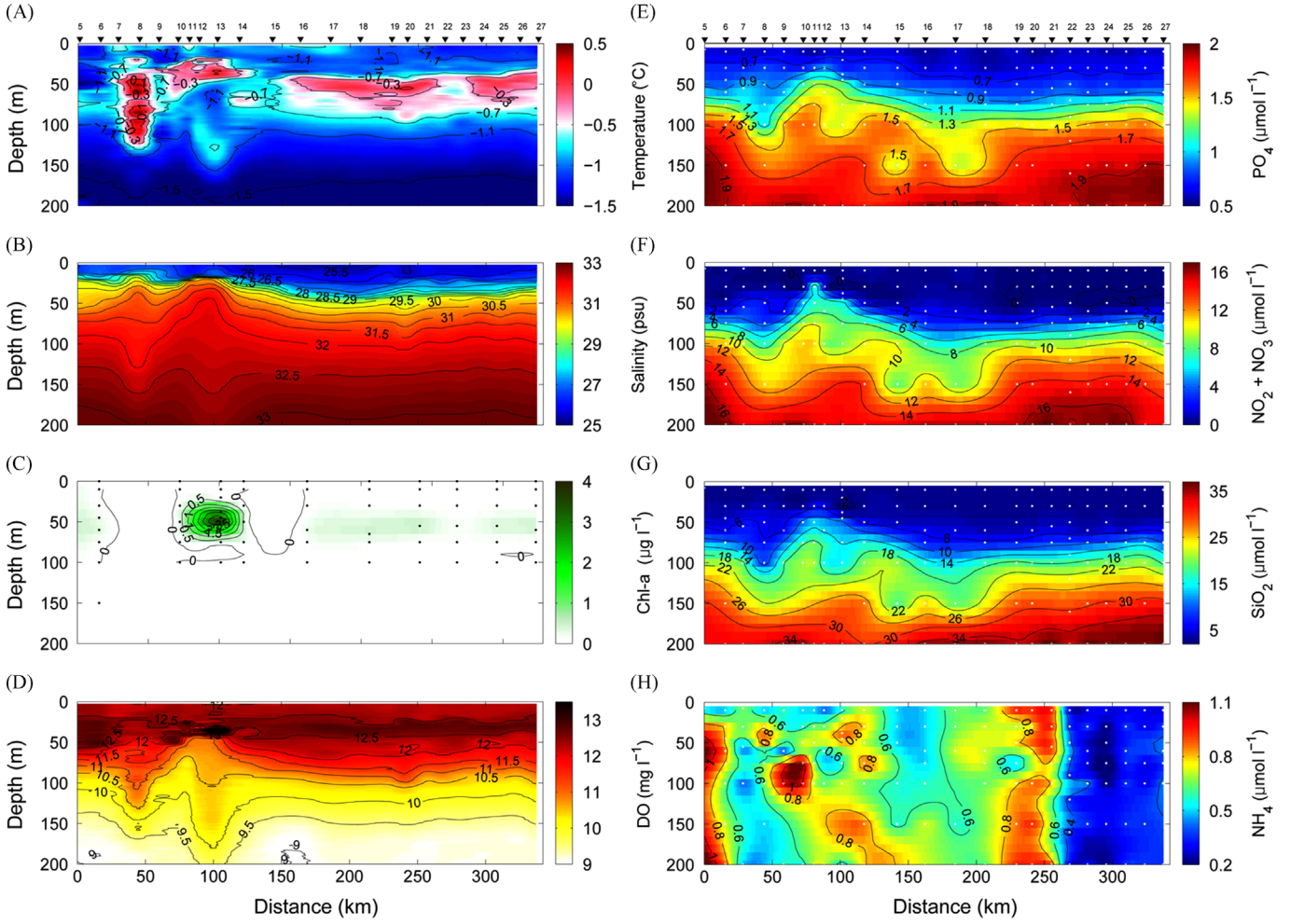

Fig. 4. Vertical section of potential temperature (a), salinity (b), chl-*a* (c), dissolved oxygen (d), phosphate (e), nitrate + nitrite (f), silicate (g), and ammonium (h).

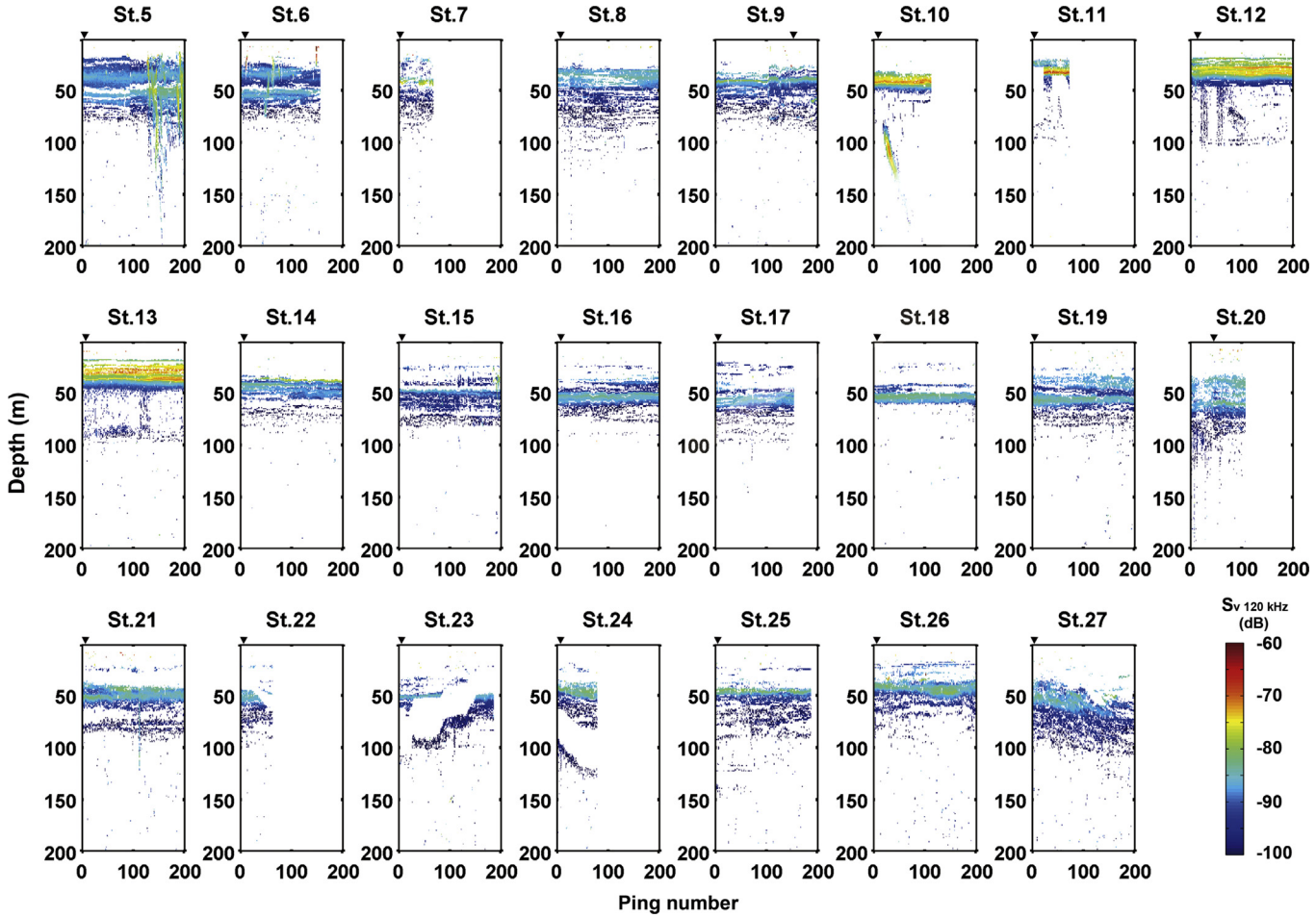

Fig. 5. Echograms of 120 kHz for the top 200 m of the water column in each station, representing the mesozooplankton. The classification is followed by dB difference method to remove the macrozooplankton and nekton (Fig. 2). The inverted triangles indicate the starting time of the CTD at each station.

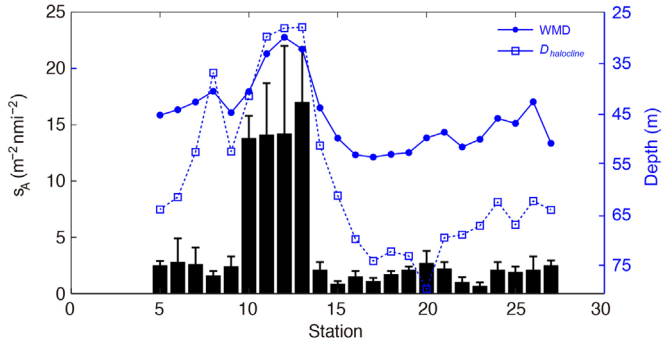

Fig. 6. Spatial variation of s_A of Arctic Copepods (vertical bar), WMD (solid line), and $D_{halocline}$ (dashed line). Note that $D_{halocline}$ is the halocline depth with 31 psu at each CTD station.

pool day and night data to exhibit the spatial variation of Arctic copepods.

The Spearman rank-correlation coefficient (r_s) was calculated for all stations to examine the environmental influences on the spatial distribution of Arctic copepods. We compared the s_A with mean temperatures, salinities, dissolved oxygen, nutrients (averaged from the surface to 100 m), and the integrated chl-*a* (from the surface to 100 m) at each station. The spatial variation of s_A was significantly correlated ($p < 0.01$) with both salinity and nitrate+nitrite. A multiple linear regression analysis was conducted and a significant correlation ($p < 0.01$) was found: an increase in the salinity and nitrate+nitrite coincided with an increased s_A related with Arctic copepods (Table 4).

4. Discussion

Multi-frequency acoustic data were used to identify the SSL of the mesozooplankton layer in the western Arctic Ocean. The SSL was mainly arisen one broad layer from 20 to 100-m depth and 80% of the SSL was concentrated between 20 and 70 m at all stations. Our ability to distinguish between mesozooplankton and other marine organisms such as fish and macrozooplankton in the acoustic data was supported by net sampling. The negative dB window values are likely to be contributed by fish with resonating gas-filled swim bladders and a dB window between 2 and 12 dB is used to identify macrozooplankton (Madureira et al., 1993; Fielding et al., 2012). The net sampling identified Arctic copepods as contributing a significant proportion of the species abundance (>90%) rather than other mesozooplankton groups (~1%) (Table 3), and s_A was highly correlated with net-sampled copepod abundance (Fig. 8). Thus, we could conclude that Arctic copepods among the mesozooplankton made the greatest contribution to the SSL and s_A.

Mesoscale eddies play important roles in controlling plankton populations (Landry et al., 1998; Vaillancourt et al., 2003), nutrient fluxes, zooplankton distribution (Llinas et al., 2009), and new production (Jenkin, 1988, McGillicuddy and Robinson, 1997; Law et al., 2001; Ledwell et al., 2008) in marine ecosystems. It would be

interesting to compare various parameters between warm and cold eddies. Cold eddies are more prevalent than warm eddies (Honjo et al., 2010). Mathis et al. (2007) calculated that a typical cold eddy with a diameter of 20 km and a depth/thickness of 75 m contains 5 μmol L^{-1} nitrate and, thus, transfers 1.25×10^8 mol of excess nitrate to the Canada Basin. Nishino et al. (2011) demonstrated that the warm eddy could transfer 8.5 times more nitrogen nutrients than a typical cold eddy. More than 100 cold eddies are expected to occur annually in the Arctic Ocean (Mathis et al., 2007), whereas large warm eddies are rare. Pacific waters are largely transported via eddies within the Alaskan coastal waters. Here, the occurrence of eddies increases from August to October by 0.2–0.3 S_v (Watanabe and Hasumi, 2009). However, at most, two large warm eddies are produced each year. Accordingly, the annual transport of excess nitrogenous nutrients by warm eddies is less than 20% of that transported by cold eddies. The present study describes the vertical and spatial distribution of the SSL for Arctic copepods in the mode-water eddies with warm-core. A single transect through an eddy might be difficult to assess the significance of the eddy for the copepods in general. However, the trend in our data suggests that a mode-water eddy with warm-core causing high nutrients and chl-*a* might provide a potential mechanism to enhance the copepod density around the Northwind Ridge, thereby affecting food webs in the Canada Basin.

Although the Canada Basin contains numerous subsurface eddies (Manley and Hunkins, 1985; Llinas et al., 2009), little is known about the impact of these eddies on the communities of Arctic mesozooplankton. Eddy-induced changes in the mesozooplankton community structure could have important implications for pelagic food webs, the transfer of particulate organic matter to deeper waters, and carbon sequestration in the ocean (Steinberg et al., 2001; Buesseler et al., 2004; Verdeny et al., 2008). It is important to understand these complex interactions in the Arctic Ocean, because mesoscale features may influence mesozooplankton biomass at spatial and temporal scales: i.e., their vertical and horizontal distribution (Andersen et al., 2011) at long-term and diel cycles. This also holds for their physiology, species succession (Wiebe et al., 1976), and carbon export (Flynn et al., 2012). This study, therefore, might provide novel insight into the mechanisms by which the mesozooplankton food web is affected by warm eddies in the western Arctic Ocean.

Vertical patterns in the SSL indicate a relatively uniform distribution over the study area with the maximum scattering layers at approximately 50-m depth. These patterns show a large portion of the SSL concentrated within the upper 100 m of water in the PSW. All locations were consistent with observations typical of the Arctic summer marine environment (Kosobokova and Hopcroft, 2010). During summer, the levels of nutrients and chl-*a* in the PSW increase relative to the other regions of the water column. Several seasonal studies showed that *C. hyperboreus* concentrates in the uppermost regions of the water column by early summer before descending to intermediate depths (~400 to 500 m) during late summer (Geynrikh et al., 1983; Ashjian et al., 2003). Unlike similar species, *C. hyperboreus* uses this migration pattern to avoid reduced salinity in the freshened surface layer. Vertical migration is not a consistent behavioral attribute but rather depends on season (Sameoto, 1984; Landry and Hassett, 1985; Vidal and Smith, 1986) or location (Williams and Conway, 1984). Most nighttime studies on Arctic zooplankton DVM were conducted in open waters (Bucklin et al., 2010; Hopcroft et al., 2010). Researchers have generally concluded that most species exhibit no clear migration pattern (Kosobokova, 1978; Groendahl and Hernroth, 1984; Longhurst et al., 1984; Sameoto, 1984; Falkenhaugh et al., 1997). Copepods that migrate between day and night in spring stop their migration when seasonal midnight sun conditions develop (Buchanan and Haney, 1980; Falkenhaugh et al., 1997). In the Arctic during summer, *C. hyperboreus*, which is a large copepod (e.g., the mean prosome length alone was described as 7–10 mm according to Wilson, 1932), does not exhibit diel vertical migration (Kosobokova, 1978; Sameoto, 1984; Hansen et al., 1990). In the present study, most stations were covered by sea ice (Table 2) with the exceptions of St. 7–9 where only limited sea ice cover existed. The mesozooplankton was primarily distributed within the PSW and was sparsely distributed in the SMW. Furthermore, the diel vertical migration is unlikely to have affected to the copepod density between day and night. These findings suggest that diel vertical migration might not have affected the vertical distribution of Arctic copepods and density distribution around the Northwind Ridge, in the western Arctic Ocean.

Spatially, the highest density of Arctic copepods was found around E2 while the density around E1 was similar to other stations outside of the warm-core eddies. The two warm-core eddies seem to have different environmental conditions. No impact was observed from changes in the nitrate- and chlorophyll-densities with the depth from the aphotic zone to the euphotic zone in E1. However, high chl-*a* concentrations and nutrient-rich waters were observed in E2 around the Northwind Ridge (Yang et al., 2015). This difference might be explained by different bathymetric conditions between the two water column structures. Bathymetric variations have a profound effect on the circulation, disruption, and redirection of flow, which enhance the degree of mixing (Richard, 1973; Pitcher et al., 2010). In regions where isobaths change abruptly, water flow is forced off the shelf by a rapid change in the orientation of the bottom bathymetry that produces eddies (Pitcher et al., 2010). The physical consequences of upwelling by abrupt changes in bathymetry are well documented and influence the pelagic ecosystem (Nelson and Hutchings, 1983; Harms and Winant, 1998; Relvas et al., 2007). Eddy-induced upwelling causes the intermittent upward flux of nutrients into the euphotic zone at magnitudes that are sufficient to balance the nutrient demand, as implied by geochemical estimates of new primary production (McGillicuddy and Robinson, 1997). Martin and Richards (2001) proposed that upwelling produced from perturbations of circular eddies is a possible mechanism for vertical nutrient transport within an eddy. Enhanced phytoplankton biomass is frequently observed at the center of an eddy (Mizobata et al., 2002; McGillicuddy et al., 2007; Ledwell et al., 2008). Upwelling transports

Table 2
System parameters calibrated for the acoustic survey.

System parameters	Simrad EK60	
Frequency (kHz)	38	120
Transmitted power (W)	2000	500
Pulse duration (ms)	1.024	1.024
2-way beam angle (dB)	−20.60	−21.00
Receiver bandwidth (kHz)	2.43	3.03
Transducer gain (dB)	22.09	26.37
3-dB beam angle (°) (along/athwart)	7.05/6.98	6.67/6.80
Absorption coefficient (dB km^{-1})	9.90	24.84
s_A Correction	−0.40	−0.38

Table 3
Relative contribution (%) of the different mesozooplankton groups to the total mesozooplankton abundance at stations around Northwind Ridge, July 2010.

Taxa	St. no.							
	6	8	13	16	21	25	27	Mean ± S.D.
Copepoda	91.7	90.3	93.6	91.2	90.7	89.8	91.1	91.2 ± 1.23
Ostracoda	0.8	1.2	2.9	0.8	1.3	1.1	1.5	1.37 ± 0.72
Polychaeta	0.9	0.8	1.7	0.6	0.9	0.8	1.2	0.99 ± 0.36
Larvacea	1.4	1.4	0.7	2.3	1.6	1.9	2.1	1.63 ± 0.53
Chaetognatha	1.6	1.3	0.1	1.8	1.8	1.4	0.7	1.24 ± 0.63
Pteropoda	1.5	1.7	0.7	2.1	1.6	1.9	1.4	1.56 ± 0.45
Ctenophora	1.2	1.7	0.2	0.3	0.7	2.0	0.8	0.99 ± 0.68
Euphusiacea	0.9	1.6	0.1	0.9	1.4	1.1	1.2	1.03 ± 0.48

Table 4
Parameters, error estimates (standard error, SE), and p value for the responses of s_A to mean salinity and nitrate+nitrite. $s_A = z + x$ salinity $+ y$ nitrate+nitrite ($n=23$, $r^2=0.63$).

Parameters	Value	SE	p
z	−112.9	37.3	< 0.01
x	3.8	1.3	< 0.01
y	1.6	0.6	< 0.01

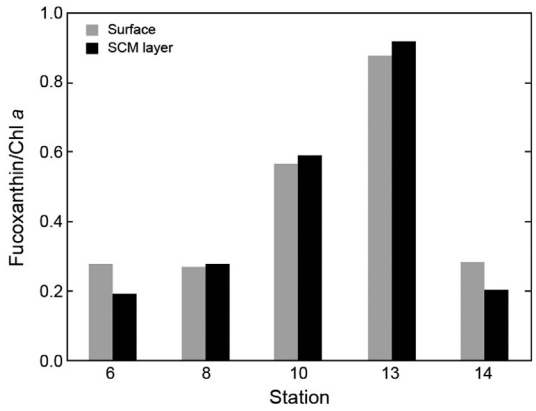

Fig. 7. Fucoxanthin to chl-*a* ratio at surface depth (grey bar) and chl-*a* maximum layer (black bar) depth between St. 6 and 14.

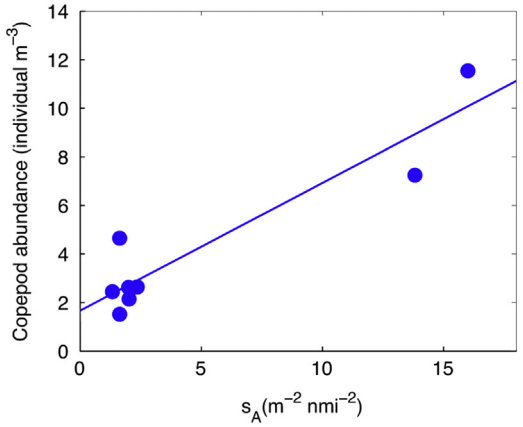

Fig. 8. Relationship between s_A and net sampled density of Arctic Copepods.

nutrient-rich water to the surface, resulting in higher phytoplankton biomass and primary production (Letelier et al., 2000; Garcon et al., 2001; Vaillancout et al., 2003).

Phytoplankton represents a primary food source for copepods. Several copepod species have long been known to feed on diatoms in the ocean (Paffenhöfer et al., 2005). Diatoms were predominant in the survey area from St. 5 to 27. We analyzed phytoplankton pigment using high performance liquid chromatography system (HPLC) according to the method of Zapata et al. (2000) to observe the ratio of fucoxanthin as an index of diatoms and chl-*a* between St. 6 and 14 (Fig. 7). The ratio was <0.3 outside E1 and between 0.6 and 0.9 inside the E2 between St. 10 and 13. This pattern indicates that diatoms were dominant in the E2 around St. 13 and that the distinct succession of dominant phytoplankton groups within the study might be related to nutrient availabilities.

Our results show that diatoms flourished due to high nutrient loads in the E2. Increased diatom levels most likely caused an increase in Arctic copepods densities because most of these crustaceans consume diatoms (Paffenhöfer et al., 2005). The bathymetry is also particularly related to densities. E2 was distributed around the steep continental slope between the Northwind Ridge and the Canada Basin (Table 1). A strong upwelling around E2 caused by bathymetry variations might have caused the high Arctic copepods densities due to the high nutrient and phytoplankton biomass. The large diatom bloom, which provides a rich food source for Arctic copepods, might have developed around the Northwind Ridge due to the supply of higher nutrient levels.

5. Conclusions

We studied the effects of a mode-water eddy with warm-core in the PSW on the mesozooplankton SSL distribution in the pelagic ecosystem around the Northwind Ridge in the western Arctic Ocean during the early summer. The SSL was mainly distributed in the PSW, and contained more than 90% of Arctic copepods at seven stations within mode-water eddies. The s_A of Arctic copepods was an order of magnitude higher around E2 than at the other stations, while no significant relationship was found for E1. E2 induced upwelling due to the shoaling of iso-halocline surfaces, allowing for the injection of nutrients into the euphotic zone, thereby, increasing the phytoplankton biomass, nutrients, and density of Arctic copepods. This suggests that the E2 is a good habitat for mesozooplankton in the Arctic Ocean due to high nutrient and phytoplankton biomass. Since eddy causes changes in the community structure of copepod populations, this may also change particulate organic matter and carbon flow generally to the deep sea.

Acknowledgments

The authors acknowledge the support and dedication of the captain and crews of *IBRV ARAON* for completing the field work with such positive energy. The authors also thank H.J. Lee, and H.D. Jun for the analyses of environmental data. H.C. Shin provided constructive comments and suggestions. We would like to sincerely thank the late K.H. Chung for his unstinting support and encouragement as a Chief Scientist during the first Arctic expedition. This research was a part of the project titled 'K-PORT (KOPRI, PM14040)', funded by the Ministry of Oceans and Fisheries (MOF), Korea. H.K. Ha was supported by the Polar Academic Program (PD14010) of KOPRI and Inha University Research Grant (INHA-49278).

References

Andersen, N.G., Nielsen, T.G., Jakobsen, H.H., Munk, P., Riemann, L., 2011. Distribution and production of plankton communities in the subtropical convergence zone of the Sargasso Sea. II. Protozooplankton and copepods. Mar. Ecol. Prog. Ser. 426, 71–86.

Armstrong, F.A.J., Steams, C.R., Strickland, J.D.H., 1967. The measurement of upwelling and subsequent biological processes by means of the Technicon Autoanalyzer and associated equipment. Deep-Sea Res. Part A. Oceanogr. Res. Pap. 14, 381–389.

Arrigo, K.R., Lowry, K.E., van Dijken, G.L., 2012. Annual changes in sea ice and phytoplankton in polynyas of the Amundsen Sea, Antarctica. Deep-Sea Res. II 71–76, 5–15.

Ashjian, C.J., Campbell, R.G., Welch, H.E., Butler, M., Van Keuren, D., 2003. Annual cycle in abundance, distribution, and size in relation to hydrography of important copepod species in the western Arctic Ocean. Deep-Sea Res. I 50, 1235–1261.

Auel, H., Hagen, W., 2002. Mesozooplankton community structure, abundance and biomass in the central Arctic Ocean. Mar. Biol. 140, 1013–1021.

Benitez-Nelson, C.R., Bidigare, R.R., Dickey, T.D., Landry, M.R., Leonard, C.L., Brown, S.L., Nencioli, F., Rii, Y.M., Maiti, K., Becker, J.W., Bibby, T.S., Black, W., Cai, W.-J., Carlson, C.A., Chen, F., Kuwahara, V.S., Mahaffey, C., McAndrew, P.M., Quay, P.D., Rappé, M.S., Selph, K.E., Simmons, M.P., Yang, E.J., 2007. Mesoscale eddies drive increased silica export in the subtropical Pacific Ocean. Science 316, 1017–1021.

Benoit-Bird, K.J., Au, W.W.L., 2004. Fine-scale diel migration dynamics of an island-associated sound-scattering layer. Deep-Sea Res. I 51, 707–719.

Brierley, A.S., Watkins, J.L., 1996. A comparison of acoustic targets at South Georgia and the South Orkney Islands during a season of krill scarcity. Mar. Ecol. Prog. Ser. 138, 51–61.
Brierley, A.S., Ward, P., Watkins, J.L., Goss, C., 1998. Acoustic discrimination of Southern Ocean zooplankton. Deep-Sea Res. II 45, 1155–1173.
Buchanan, C., Haney, J.F., 1980. Vertical migrations of zooplankton in the Arctic: a test of the environmental controls. In: Kerfoot, W.C. (Ed.), Evolution and Ecology of Zooplankton Communities. University Press, Hanover, pp. 69–79.
Bucklin, A., Hopcroft, R.R., Kosobokova, K.N., Nigro, L.M., Ortman, B.D., Jennings, R. M., Sweetman, C.J., 2010. DNA barcoding of Arctic Ocean holozooplankton for species identification and recognition. Deep-Sea Res. II 57, 40–48.
Buesseler, K.O., Andrews, J.E., Pike, S.M., Charette, M.A., 2004. The effects of iron fertilization on carbon sequestration in the Southern Ocean. Science 304, 414–417.
CCAMLR, 2010. Report of the Fifth Meeting of the Subgroup on Acoustic Survey and Analysis methods. SC-CCAMLR-XXIX/6.
Campbell, R.G., Sherr, E.B., Ashjian, C.J., Plourde, S., Sherr, B.F., Hill, V., Stockwell, D. A., 2009. Mesozooplankton prey preference and grazing impact in the western Arctic Ocean. Deep-Sea Res. II 56, 1274–1289.
Clay, C.S., Medwin, H., 1977. Acoustical Oceanography: Principles and Applications. John Wiley & Sons, New York, pp. 216–252.
Conover, R.J., 1988. Comparative life histories in the genera *Calanus* and *Neocalanus* in high-latitudes of the northern hemisphere. Hydrobiologia 167, 127–142.
Conover, R.J., Huntley, M., 1991. Copepods in ice-covered seas distribution, adaptations to seasonally limited food, metabolism, growth patterns and life cycle strategies in polar seas. J. Mar. Syst. 2, 1–41.
Cottier, F.R., Tarling, G.A., Wold, A., Falk-Petersen, S., 2006. Unsynchronised and synchronised vertical migration of zooplankton in a high Arctic fjord. Limnol. Oceanogr. 51, 2586–2599.
Dvoretsky, V.G., Dvoretsky, A.G., 2010. Checklist of fauna found in zooplankton samples from the Barents Sea. Polar Biol. 33, 991–1005.
Falkenhaugh, T., Tande, K.S., Semenova, T., 1997. Diel, seasonal and ontogenetic variations in the vertical distributions of four marine copepods. Mar. Ecol. Prog. Ser. 149, 105–119.
Falk-Petersen, S., Pedersen, G., Kwasniewski, S., Hegseth, E.N., Hop, H., 1999. Spatial distribution and life cycle timing of zooplankton in the marginal ice zone of the Barents Sea during the summer melt season in 1995. J. Plankton Res. 21, 1249–1264.
Falk-Petersen, S., Leu, E., Berge, J., Kwasniewski, S., Nygard, H., Rostad, A., Keskinen, E., Thormar, J., von Quillfeldt, C., Wold, A., Gulliksen, B., 2008. Vertical migration in high Arctic waters during Autumn 2004. Deep-Sea Res. II 55, 20–21.
Fielding, S, Watkins, J.L., Collins, M.A., Enderlein, P., Venables, H.J., 2012. Acoustic determination of the distribution of fish and krill across the Scotia Sea in spring 2006, summer 2008 and autumn 2009. Deep-Sea Res. II 59–60, 173–188.
Flagg, C.N., Smith, S.L., 1989. On the use of acoustic Doppler current profiler to measure zooplankton abundance. Deep-Sea Res. 36, 455–474.
Flynn, K.J., Blackford, J.C., Baird, M.E., Raven, J.A., Clark, D.R., Beardall, J., Brownlee, C., Fabian, H., Wheeler, G.L., 2012. Changes in pH at the exterior surface of plankton with ocean acidification. Nat. Clim. Change – Lett. 2, 510–513.
Foote, K.G., Stanton, T.K., 2000. Acoustical methods. In: Harris, R.P., Wiebe, P.H., Lentz, J., Skjoldal, H.R., Huntley, M. (Eds.), ICES Zooplankton Methodology Manual. Academic Press, New York, pp. 223–258.
Garcon, V.C., Oschlies, A., Doney, S.C., McGillicuddy, D.J., Waniek, J., 2001. The role of mesoscale variability on plankton dynamics in the North Atlantic. Deep-Sea Res. II 48, 2199–2226.
Geynrikh, A.K., Kosobokova, K.N., Rudyakov, Y.A., 1983. Seasonal variations in the vertical distribution of some prolific copepods of the Arctic Basin. Can. J. Fish. Aquat. Sci. 4925, 1–22.
Grasshoff, K., Erhardt, M., Kremling, K., 1983. Methods of Seawater Analysis. Verlag Chemie, Weinheim, pp. 139–142.
Grebmeier, J.M., Harvey, H.R., 2005. The Western Arctic Shelf-Basin Interactions (SBI) Project: an overview. Deep-Sea Res. II 52, 3109–3115.
Groendahl, F., Hernroth, L., 1984. Vertical distribution of copepods in the Eurasian part of the Nansen Basin, Arctic Ocean. Syllogeus 58, 311–320.
Hansen, B., Berggreen, U.C., Tande, K.S., Eilertsen, H.C., 1990. Post-bloom grazing by *Calanus glacialis*, *C. finmarchicus* and *C. hyperboreous* in the region of the Polar Front, Barents Sea. Mar. Biol. 104, 5–14.
Harms, S., Winant, C.D., 1998. Characteristic patterns of the circulation in the Santa Barbara Channel. J. Geophys. Res. Oceans 103, 3041–3065.
Hassel, A., Skjoldal, H.R., Gjosaeter, H., Loeng, H., Omli, L., 1991. Impact of grazing from capelin (*Mallotus villosus*) on zooplankton: a case study in the northen Barents Sea in August 1985. Polar Res. 10, 371–388.
Hopcroft, R.R., Kosobokova, K.N., Pinchuk, A.I., 2010. Zooplankton community patterns in the Chukchi Sea during summer 2004. Deep-Sea Res. II 57, 27–39.
Honjo, S., Krishfield, R.A., Eglinton, T.I., Manganini, S.J., Kemp, J.N., Doherty, K., Hwang, J., McKee, T.K., Takizawa, T., 2010. Biological pump processes in the cryopelagic and hemipelagic Arctic Ocean: Canada Basin and Chukchi Rise. Prog. Oceanogr. 85, 137–170.
Iken, K., Bluhm, B., Dunton, K., 2010. Benthic food-web structure under differing water mass propoerties in the southern Chukchi Sea. Deep-Sea Res. II 57, 71–85.
Jenkin, W.J., 1988. Nitrate flux into the euphotic zone near Bermuda. Nature 331, 521–522.
Kang, M., Furusawa, M., Miyashita, K., 2002. Effective and accurate use of difference in mean volume backscattering strength to identify fish and plankton. ICES J. Mar. Sci. 59, 794–804.
Kosobokova, K.N., 1978. Diurnal vertical distribution of *Calanus hyperboreus* Kroyer and *Calanus glacialis* Jaschnov in the Central Polar Basin. Oceanology 18, 476–480.
Kosobokova, K., Hirche, H.-J., 2000. Zooplankton distribution across the Lomonosov Ridge, Arctic Ocean: species inventory, biomass and vertical structure. Deep-Sea Res. I 47, 2029–2060.
Kosobokova, K.N., Hopcroft, R.R., 2010. Diversity and vertical distribution of mesozooplankton in the Arctic's Canada Basin. Deep-Sea Res. II 57, 96–110.
La, H.S., Lee, H., Fielding, S., Kang, D., Ha, H.K., Atkinson, A., Park, J., Siegel, V., Lee, S., Shin, H.C., 2015. High density of ice krill (*Euphausia crystallorophias*) in the Amundsen Sea Coastal Polynya, Antarctica. Deep-Sea Res. I 95, 75–84.
Landry, M.R., Hassett, R.P., 1985. Time scales in behavioral, biochemical and energetic adaptations to food-limiting conditions by a marine copepod. Arch. Hydrobiol. Beih Ergebn Limnol. 21, 209–221.
Landry, M.R., Brown, S.L., Campbell, L., Constantinou, J., Liu, H., 1998. Spatial patterns in phytoplankton growth and microzooplankton grazing in the Arabian Sea during monsoon forcing. Deep-Sea Res. II 45, 2368–2523.
Law, C.S., Martin, A.P., Liddicoat, M.I., Watson, A.J., Richards, K.J., Woodward, E.M.S., 2001. A Lagrangian SF_6 tracer study of an anticyclonic eddy in the North Atlantic: patch evolution, vertical mixing and nutrient supply to the mixed layer. Deep-Sea Res. II 48, 705–724.
Ledwell, J.R., McGillicuddy, D.J., Anderson, L.A., 2008. Nutrient flux into an intense deep chlorophyll layer in a mode-water eddy. Deep-Sea Res. II 55, 1139–1160.
Letelier, R.M., Kal, D.M., Abbott, M.R., Flament, P., Frielich, M., Lukas, R., Strub, T., 2000. Role of late winter mesoscale events in the biogeochemical variability of the upper water column of the North Pacific Subtropical Gyre. J. Geophys. Res. 105, 28723–28739.
Llinas, L., Pickart, R.S., Mathis, J.T., Smith, S.L., 2009. Zooplankton inside an Arctic Ocean cold-core eddy: probable origin and fate. Deep-Sea Res. II 56, 1290–1304.
Longhurst, A., Sameoto, D., Herman, A., 1984. Vertical distribution of Arctic zooplankton in summer: eastern Canadian Archipelago. J. Plankton Res. 6, 137–168.
Lonne, O.J., Gulliksen, B., 1989. Size, age and diet of polar cod, *Boreogadus saida* (Lepechin 1773), in ice covered waters. Polar Biol. 9, 187–191.
Madureira, L.S.P., Everson, I., Murphy, E.J., 1993. Interpretation of acoustic data at two frequencies to discriminate between Antarctic krill (*Euphausia superba* Dana) and other scatterers. J. Plankton Res. 15, 787–802.
Manley, T.O., Hunkins, K., 1985. Mesoscale eddies of the Arctic Ocean. J. Geophys. Res. 90, 1978–2012.
Martin, A.P., Richards, K.J., 2001. Mechanisms for vertical nutrient transport within a North Atlantic mesoscale eddy. Deep-Sea Res. II 48, 757–773.
Maslanik, J.A., Serreze, M.C., Agnew, T., 1999. On the record reduction in 1998 western Arctic sea ice cover. Geophys. Res. Lett. 26, 1905–1908.
Mathis, J.T., Pickart, R.S., Hansell, D.A., Kadko, D., Bates, N.R., 2007. Eddy transport of organic carbon and nutrients from the Chukchi Shelf: impact on the upper halocline of the western Arctic Ocean. J. Geophys. Res. 112, C05011.
Manley, T.O., Hunkins, K., 1985. Mesoscale eddies of the Arctic Ocean. J. Geophys. Res. 90, 4911–4930.
McGillicuddy, D.J., Robinson, A.R., 1997. Eddy-induced nutrient supply and new production in the Sargasso Sea. Deep-Sea Res. I 44, 1427–1450.
McGillicuddy, D.J., Johnson, R., Siegel, D.A., Michaels, A.F., Bates, N.R., Knap, A.H., 1999. Mesoscale variations of biogeochemical properties in the Sargasso Sea. J. Geophys. Res. 104, 13381–13394.
McGillicuddy, D.J., Anderson, L.A., Bates, N.R., Bibby, T., Buesseler, K.O., Carlson, C., Davis, C.S., Ewart, C., Falkowski, P.G., Goldthwait, S.A., Hansell, D.A., Jenkins, W. J., Johnson, R., Kosnyrev, V.K., Ledwell, J.R., Li, Q.P., Siegel, D.A., Steinberg, D.K., 2007. Eddy–wind interactions stimulate extraordinary mid-ocean plankton blooms. Science 316, 1021–1026.
McManus, M.A., Benoit-Bird, K.J., Woodson, C.B., 2008. Behavior exceeds physical forcing in the diel horizontal migration of a midwater sound-scattering layer in Hawaiian waters. Mar. Ecol. Prog. Ser. 365, 91–101.
Mizobata, K., Saitoh, S.I., Shiomoto, A., Miyamura, T., Shiga, N., Imai, K., Toratani, M., Kajiwara, Y., Sasaoka, K., 2002. Bering Sea cyclonic and anticyclonic eddies observed during summer 2000 and 2001. Prog. Oceanogr. 55, 65–75.
Muench, R.D., Gunn, J.T., Whitledge, T.E., Schlosser, P., Smethie, W., 2000. An Arctic Ocean cold core eddy. J. Geophys. Res. 105 (C10), 23997–24006.
Munchow, A., Carmack, E.C., 1997. Synoptic flow and density observations near an arctic shelf break. J. Phys. Oceanogr. 27, 1402–1419.
Myriax, 2012. Help file 5.20 for Echoview [Internet]. Myriax, Hobart, TAS, AU. ⟨http://support.echoview.com/WebHelp/Echoview.htm⟩ (accessed 06.04.11.).
Nelson, G., Hutchings, L., 1983. The Benguela upwelling area. Prog. Oceanogr. 12, 333–356.
Nishino, S., Itoh, M., Kawaguchi, Y., Kikuchi, T., Aoyama, M., 2011. Impact of an unusually large warm-core eddy on distributions of nutrients and phytoplankton in the southwestern Canada Basin during late summer/early fall 2010. Geophys. Res. Lett. 38 (L16602), 1–6.
Parsons, T.R., Maita, Y., Lalli, C.M., 1984. A Manual of Chemical and Biological Methods for Seawater Analysis. Pergamon Press, Oxford p. 173.
Paffenhöfer, G.A., et al., 2005. Colloquium on diatom–copepod interactions. Mar. Ecol. Prog. Ser. 286, 293–305.
Pitcher, G.C., Figueiras, F.G., Hickey, B.M., Moita, M.T., 2010. The physical oceanography of upwelling systems and development of harmful algal blooms. Prog. Oceanogr. 85, 5–32.
Plourde, S., Campbell, R.G., Ashjian, C.J., Stockwell, D., 2005. Seasonal and regional patterns in egg production of *Calanus glacialis*/*marshallae* in the Chukchi and Beaufort Seas during spring and summer 2002. Deep-Sea Res. II 52, 3411–3426.

Rabindranath, A., Daase, M., Falk-Petersen, S., Wold, A., Wallace, M.I., Berge, J., Brierly, A.S., 2011. Seasonal and diel vertical migration of zooplankton in the High Arctic during the autumn midnight sun of 2008. Mar. Biodiversity 41, 365–382.
Relvas, P., Peliz, A., Oliveira, P.B., da Silva, J., Dubert, J., Barton, E.D., Santos, A.M.P., 2007. Physical oceanography of the western Iberia ecosystem: latest views 18 and challenges. Prog. Oceanogr. 74, 149–173.
Richard, W.G., 1973. The effect of Bathymetry on the coastal upwelling of homogeneous water. J. Phys. Oceanogr. 3, 47–56.
Riser, C.W., Wassmann, P., Reigstad, M., Seuthe, L., 2008. Vertical flux regulation by zooplankton in the northern Barents Sea during Arctic spring. Deep-Sea Res. II 55, 2320–2329.
Roe, H.S.J., Angel, M.V., Badcock, J., Domanski, P., James, P., Pugh, P.R., Thurston, M. H., 1984. The diel migrations and distributions within a mesopelagic community in the North East Atlantic. 1. Introduction and sampling procedures. Prog. Oceanogr. 13, 245–260.
Sameoto, D.D., 1984. Environmental factors influencing diurnal distribution of zooplankton and ichthyoplankton. J. Plankton Res. 6, 767–792.
Santora, J.A., Ralston, S., Sydeman, W.J., 2011. Spatial organization of krill and seabirds in the central California Current. ICES J. Mar. Sci. 68, 1391–1402.
Shimada, K., Kamoshida, T., Itoh, M., Nishino, S., Carmack, E., McLaughlin, F., Zimmerman, S., Proshutinsky, A., 2006. Pacific Ocean inflow: influence on catastrophic reduction of sea ice cover in the Arctic Ocean. Geophys. Res. Lett. 33, L08605.
Simmonds, E.J., MacLennan, D.N., 2005. Fisheries Acoustics: Theory and Practice. Blackwell Science, Oxford, p. 60.
Sirenko, B.I., 2001. List of species of free-living invertebrates of Eurasian Arctic Seas and adjacent deep waters. Russ. Acad. Sci. Explor. Fauna Sea 51, 1–129.
Steinberg, D.K., Carlson, C.A., Bates, N.R., Johnson, R.J., Michaels, A.F., Knap, A.H., 2001. Overview of US JGOFS Bermuda Atlantic Time-series Study (BATS): a decade-scale look at ocean biology and biogeochemistry. Deep-Sea Res. II Top. Stud. Oceanogr. 48, 1405–1448.
Vaillancourt, R.D., Marra, J., Seki, M.P., Parsons, M.L., Bidigare, R.R., 2003. Impact of a cyclonic eddy on phytoplankton community structure and photosynthetic competency in the subtropical North Pacific Ocean. Deep-Sea Res. I 50, 829–847.
Verdeny, E., Masque, P., Maiti, K., Garcia-Orellana, J., Bruach, J.M., Mahaffey, C., Benitez-Nelson, C.R., 2008. Particle export within cyclonic Hawaiian lee eddies derived from ^{210}Pb–^{210}Po disequilibrium. Deep-Sea Res. II 55, 1461–1472.
Vidal, J., Smith, S.L., 1986. Biomass, growth and development of populations of herbivorous zooplankton in the southeastern Bering Sea during spring. Deep-Sea Res. II 33, 523–556.
Watkins, J.L., Brierley, A.S., 1996. A post-processing technique to remove background noise from echo-integration data. ICES J. Mar. Sci. 53, 339–344.
Walsh, J.J., 1995. DOC storage in Arctic Seas: the role of continental shelves. Coast. Estuar. Stud. 49, 203–230.
Watanabe, E., Hasumi, H., 2009. Pacific water transport in the western Arctic Ocean simulated by an eddy-resolving coupled sea ice-ocean model. J. Phys. Oceanogr. 39, 2194–2211.
Weslawski, J.M., Stempniewicz, L., Mehlum, F., Kwasniewski, S., 1999. Summer feeding strategy of the little auk (*Alle alle*) from Bjornoya, Barents Sea. Polar Biol. 21, 129–134.
Wiebe, P.H., Burt, K.H., Boyd, S.H., et al., 1976. A multiple opening/closing net and environmental sensing system for sampling zooplankton. J. Mar. Res. 34, 313–326.
Williams, R., Conway, D.V.P., 1984. Vertical distribution, and seasonal and diurnal migration of *Calanus helgolandicus* in the Celtic Sea. Mar. Biol. 79, 63–73.
Wilson, C.B., 1932. The Copepods of the Woods Hole region, Massachusetts. US Government Printing Office, Washington, DC.
Woodgate, R.A., Weingartner, T.J., Lindsay, R., 2012. Observed increases in Bering Strait oceanic fluxes from the Pacific to the Arctic from 2001 to 2011 and their impacts on the Arctic Ocean water column. Geophy. Res. Lett. 39, L24603. http://dx.doi.org/10.1029/2012GL054092.
Yang, E.J., Ha, H.K., Chung, K.H., Kang, S.H., 2015. Microzooplankton community structure and grazing impact on major phytoplankton in the Chukchi Sea and the western Canada Basin, Arctic Ocean. Deep-Sea Res. II 120, 91–102. http://dx.doi.org/10.1016/j.dsr2.2014.05.020.
Zapata, M., Rodriguez, F., Garrido, J.L., 2000. Separation of chlorophylls and carotenoids from marine phytoplankton: a new HPLC method using a reversed phase C8 column and pyridine-containing mobile phases. Mar. Ecol. Prog. Ser. 195, 29–45.
Zimmerman, R.A., Biggs, D.C., 1999. Patterns of distribution of sound-scattering zooplankton in warm- and cold-core eddies in the Gulf of Mexico, from a narrowband acoustic Doppler current profiler survey. J. Geophys. Res. 104, 5251–5262.